Journal of Magnetic Resonance **142,** 139–144 (2000)
Article ID jmre.1999.1921, available online at http://www.idealibrary.com on IDEAL®

Detection of Anisotropic Hyperfine Transitions in Zero Magnetic Field Using Field-Cycling Techniques

G. Sturm, D. Kilian, A. Lötz,[1] and J. Voitländer

Institut für Physikalische Chemie, Universität München, Butenandtstraße 5-13, D-81377 Munich, Germany

Received May 11, 1999; revised August 17, 1999

For the first time, we describe the detection of hyperfine transitions in zero magnetic field using field-cycling techniques and pulsed EPR spectroscopy. The sample investigated was coal, which shows an anisotropic electron spin–^{13}C hyperfine interaction. © 2000 Academic Press

Key Words: **pulsed field-cycled ENDOR spectroscopy; zero-field ENDOR spectroscopy; zero-field resonance spectroscopy; field-cycling EPR; bridged loop–gap resonator.**

INTRODUCTION

The resolution enhancement of inhomogeneously broadened powder spectra is one of the major goals in modern EPR and ENDOR spectroscopy. This line broadening, due to the magnetic inequivalence of otherwise identical spins, can partly be removed in modern high-field EPR experiments (*1*). A complete removal of inhomogeneous line broadening is possible in zero-field EPR spectroscopy (zero-field resonance, ZFR (*2*)), because the zero-field transitions are independent of the individual orientations of the crystallites in the powder sample. Yet the sensitivity of ZFR is only satisfying for large zero-field splittings. It is, however, possible to perform the excitation of the transitions of interest in zero field and to detect the effect of this excitation on the spin system in a high magnetic field which combines the resolution of ZFR and the sensitivity of X-band EPR.

An experiment of this kind was proposed by Abragam in 1956 (*3*). A review of Fourier transform time-domain zero-field NMR and NQR experiments with the same motivation was given by Zax *et al.* (*4*). However, to the best of our knowledge, there are only five experimental papers on field-cycling EPR. The first field-cycled ENDOR experiment was described in 1994 by Krzystek *et al.*, (*5*), who used a CW detection of the electronic magnetization. The pulsed detection introduced by us (*6, 7*) extends the general usability of field-cycled ENDOR. Recently, we reported the first detection of hyperfine transitions using field-cycling techniques (*8*). A review of this new field was given by us in (*9*). The experiment described here shows the resolution enhancement of field-cycled ENDOR spectroscopy for the detection of anisotropic hyperfine transitions in zero field.

[1] To whom correspondence should be addressed. E-mail: aloetz@olymp.cup.uni-muenchen.de.

PRINCIPLE OF THE EXPERIMENT

The time scale of a field-cycled ENDOR experiment is shown in Fig. 1. The external magnetic field is switched *adiabatically* in a time t_{switch} from a high magnetic field $\mathbf{B}_0$ to zero after complete spin relaxation in a time $t_{\text{high field}}$. This results in a reduction of the spin temperature since the entropy of the spin system remains constant on account of the adiabatic transit (*10*). In zero-field relaxation, processes with a time constant T_{1D} can take place, because the temperature of the spin system and that of the lattice are different. If the magnetic field is restored to $\mathbf{B}_0$ after a time short compared to T_{1D}, the magnetization may return to its original high-field value. Exciting the transitions of interest in zero field with RF irradiation for a time t_{exciting} destroys a part of the magnetization. This change of the magnetization can be observed after the return to high field by a "detector" spin system.

Experiments of this kind have been known for a long time in NQR double-resonance spectroscopy (*level crossing*, DRLC (*11*)), in which protons are usually used as detectors for transitions of adjacent quadrupole nuclei. Similarly, in a field-cycled ENDOR experiment, electrons are used as detectors for hyperfine transitions or nuclear quadrupole transitions in zero magnetic field. Two adiabatic conditions must be met: (a) The complete cycle time t_{cycle} must be short compared to the longitudinal high-field and zero-field relaxation times T_1 and T_{1D}; i.e., $t_{\text{cycle}} \ll T_1, T_{1D}$. (b) The switching rate of the magnetic field must fulfill the condition $|\mathbf{B}_0 \times d\mathbf{B}_0/dt|/B_0^2 \ll \gamma B_0$ for a reversible cycle; that means field switching must not be too fast. The adiabatic condition (b) is easily satisfied for electrons, but condition (a) can only be met with rapidly switched air-core magnets due to the short electronic spin–lattice relaxation times, which are typically of the order of a few milliseconds at 4.2 K. Our field-cycling spectrometer (*12*) accordingly has a switching time t_{switch} of 0.7 ms for the transit from 0.33 T to zero. The zero-field dwell time t_{dwell} must be chosen long enough to ensure ENDOR excitation and short enough to

1090-7807/00 $35.00

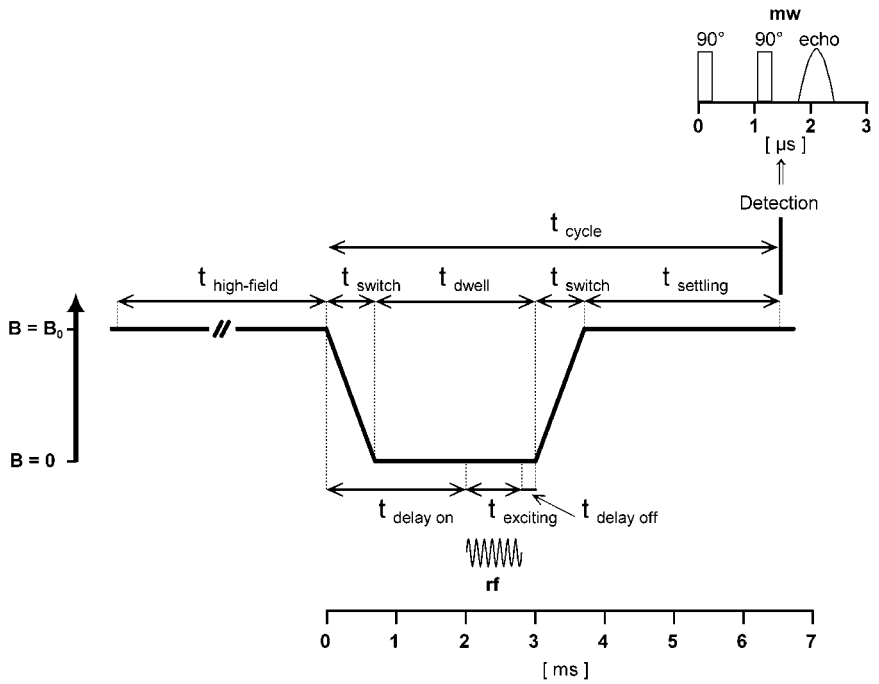

FIG. 1. Principle of a field-cycling ENDOR experiment. The spin system can be excited with radiofrequency irradiation in zero field. See text for details.

recover a part of the longitudinal magnetization at the end of the cycle. The detection of this magnetization by electron spin echoes starts immediately after settling of the magnetic field (t_{settling}). This is mandatory for substances with rapid high-field relaxation in order to gain information on the magnetization change during t_{dwell}. The ENDOR excitation in zero field should not start immediately at the beginning of the zero-field period because of a small, exponentially decaying transient current in the air-core magnet after the cycling which is inherent to all field-cycling spectrometers. A delay time $t_{\text{delay on}}$ should be used, which must be chosen in conformity with the T_{1D} time.

RESULTS AND DISCUSSION

A coal sample (impregnating pitch HL, VfT AG Castrop-Rauxel) was used in our experiments. This sample, with 93% carbon content, is a complex mixture of aromatic and heterocyclic hydrocarbons. Although a better defined sample would have been of advantage, impregnating pitch HL was used because of its long phase-memory time T_M of about 600 ns at room temperature and 900 ns in liquid helium. Such long T_M times were necessary because our ESP 380 EPR spectrometer is not equipped with a pulsed amplifier and thus is restricted to the microwave power of the klystron. Ninety degree pulses take 250–300 ns. This prevents the detection of echoes from most other samples.

Figure 2 (lower trace) shows the pulsed field-cycled ENDOR spectrum of impregnating pitch HL at 4.2 K, published by us earlier (*8*, *9*). The magnetic field dropped within 0.5 ms from high field to zero field. In zero field the sample was irradiated for 800 μs with a frequency stepped by an equal increment of 50 kHz after each cycle. The echo intensity was monitored 2.5 ms after switching back to high field. No accumulation was performed. Seventy percent of the high-field

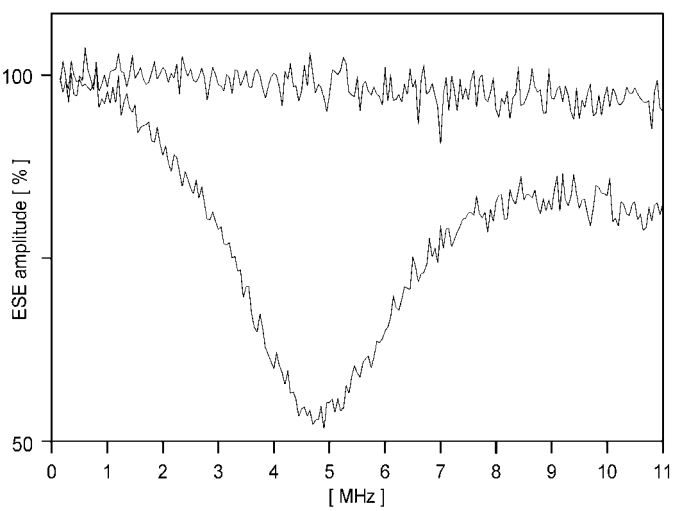

FIG. 2. Pulsed field-cycled ENDOR spectrum of a coal sample at 4.2 K obtained with our old field-cycling solenoid (see text). Echo intensity versus RF irradiation frequency in MHz. Two low-power microwave pulses of 300 ns length were used for the detection. (Bottom) Recovered EPR amplitude after irradiation in zero field. No accumulation. (Top) Equal experimental conditions, yet without RF irradiation. Experimental parameters: $t_{\text{high field}}$ = 2 s, t_{switch} = 0.5 ms, $t_{\text{delay on}}$ = 0.5 ms, t_{exciting} = 0.8 ms, $t_{\text{delay off}}$ = 0.2 ms, t_{settling} = 2 ms.

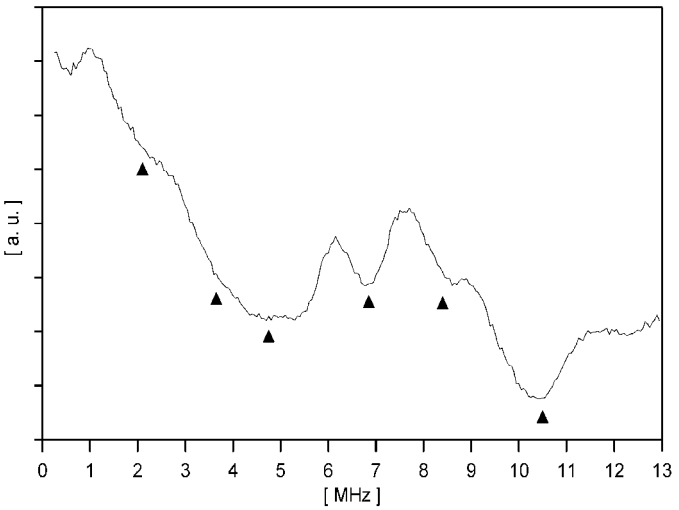

FIG. 3. Pulsed field-cycled ENDOR spectrum of a coal sample at 1.6 K obtained with our new field-cycling solenoid and compensation of the stray magnetic field (see text). Echo intensity versus RF irradiation frequency in MHz. Two low-power microwave pulses of 250 ns length were used for the detection. Four accumulations. The arrows indicate the calculated line positions for the ^{13}C hyperfine tensor given in the text. Experimental parameters: $t_{\text{high field}} = 3$ s, $t_{\text{switch}} = 0.7$ ms, $t_{\text{delay on}} = 2$ ms, $t_{\text{exciting}} = 0.8$ ms, $t_{\text{delay off}} = 0.2$ ms, $t_{\text{settling}} = 2.8$ ms.

EPR signal is lost due to spin–lattice relaxation in zero field. A comparison with the upper trace of Fig. 2, obtained without RF irradiation in zero field, shows the remarkably strong ENDOR effect of 50%. Only one broad ENDOR line can be seen in this spectrum, similar to the broad powder patterns found in room temperature HYSCORE experiments of a similar sample and assigned to ^{1}H and ^{13}C hyperfine couplings (*13*). This spectrum is the first field-cycled ENDOR spectrum of a nucleus with direct magnetic coupling to the electron spin.

However, the potential of this method to enhance spectral resolution was not yet shown. We therefore improved our magnetic field-cycling apparatus. With a new field-cycling solenoid, it is now possible to perform experiments at 1.6 K. Thus a longer $t_{\text{delay on}}$ can be chosen as the result of the longer T_{1D} time at 1.6 K compared to 4.2 K. The second improvement is an effective compensation of the Earth's magnetic field and the stray field of a conventional EPR magnet located in the same laboratory.

The field-swept electron spin–echo spectrum of impregnating pitch HL at 1.6 K consists of a transition with g value of practically that of the free electron and a width at half-height of approximately 0.9 mT. An indication of a 0.1 mT splitting is visible at the top of the line. Additionally, a broad transition of 4 mT width appears at higher field. Only the intense, narrower transition yielded field-cycled ENDOR spectra. Figure 3 shows the improved resolution. In spite of the low natural abundance of ^{13}C, this spectrum can tentatively be understood by assuming an $S = \frac{1}{2}$, $I = \frac{1}{2}$ spin system and fitting the six transitions of the zero-field Hamiltonian $\mathcal{H} = S \cdot A \cdot I$, which results in an anisotropic ^{13}C hyperfine tensor (15.25, 5.75, 1.55) MHz (see Table 1 for the eigenfunctions, eigenvalues, and calculated zero-field transitions). This interpretation is supported by the ^{13}C hyperfine tensor of (16, 6, 1) MHz for impregnating pitch HL measured by Höfer (*13*) in room temperature HYSCORE experiments with less accurate determination of the components of the ^{13}C tensor. The signals obtained by Höfer are centered at the ^{1}H and ^{13}C nuclear Larmor frequencies and the amplitudes are weighted by the anisotropy of the hyperfine couplings. In contrast to these high-field experiments, ^{13}C hyperfine couplings and ^{1}H hyperfine couplings are expected in the same frequency region in zero field so that the transitions observed between 0 and 13 MHz might represent both ^{13}C and ^{1}H hyperfine couplings. From the paper by Höfer (*13*), a broad and structureless ^{1}H signal is expected in zero field on account of the wide distribution of ^{1}H hyperfine tensors with small anisotropies. This ^{1}H transition should carry signals from ^{13}C with resolvable, anisotropic hyperfine interaction as indeed visible in the experimental field-cycling spectrum (Fig. 3). The proton signal extends to still higher frequencies than shown in Figs. 2 and 3, with another transition at 22.5 MHz. This is why the signal does not return to the basis line in both figures.

The pulsed ENDOR spectrum of pitch HL in high field mirrors the low natural isotopic abundance of ^{13}C (*14*). In the ESEEM experiments, the high sensitivity of ^{13}C detection can be explained by the high anisotropy of the hyperfine interaction, which leads to a large modulation depth parameter. In the field-cycled ENDOR experiment, a number of reasons can be thought of for the sensitivity to ^{13}C, among them specific relaxation rates in zero field for the different interactions. These are obviously visible on comparison of the spectra at 4.2 (Fig. 2) and 1.6 K (Fig. 3) in the range above 5 MHz.

TABLE 1
Hyperfine Transitions for an $S = \frac{1}{2}$, $I = \frac{1}{2}$ System in Zero Magnetic Field

Eigenfunctions	Eigenvalues
$\|1\rangle = \frac{1}{\sqrt{2}}[\|++\rangle + \|--\rangle]$	$E_1 = \frac{1}{4}(A_{xx} - A_{yy} + A_{zz})$
$\|2\rangle = \frac{1}{\sqrt{2}}[\|++\rangle - \|--\rangle]$	$E_2 = \frac{1}{4}(-A_{xx} + A_{yy} + A_{zz})$
$\|3\rangle = \frac{1}{\sqrt{2}}[\|+-\rangle + \|-+\rangle]$	$E_3 = \frac{1}{4}(A_{xx} + A_{yy} - A_{zz})$
$\|4\rangle = \frac{1}{\sqrt{2}}[\|+-\rangle - \|-+\rangle]$	$E_4 = \frac{1}{4}(-A_{xx} - A_{yy} - A_{zz})$

Fit parameters: $A_{xx} = 15.25$ MHz, $A_{yy} = 5.75$ MHz, $A_{zz} = 1.55$ MHz

$\|1\rangle \Leftrightarrow \|3\rangle$	$\|2\rangle \Leftrightarrow \|4\rangle$	$\|1\rangle \Leftrightarrow \|2\rangle$	$\|2\rangle \Leftrightarrow \|3\rangle$	$\|1\rangle \Leftrightarrow \|4\rangle$	$\|3\rangle \Leftrightarrow \|4\rangle$
2.10 MHz	3.65 MHz	4.75 MHz	6.85 MHz	8.40 MHz	10.50 MHz

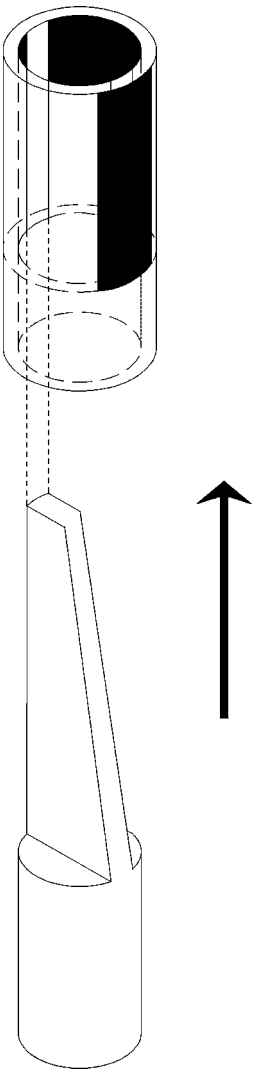

FIG. 4. Tool made from a steel rod for the construction of a bridged loop–gap resonator. The steel rod has the same diameter as the inner diameter of the BLGR. The outer structure of the resonator is scratched with a sharp knife.

CONCLUSION

The first pulsed field-cycled ENDOR spectrum of a coal sample with resolved anisotropic ^{13}C hyperfine structure is presented. Since the longitudinal relaxation times of this sample are typical for an organic radical, pulsed field-cycled ENDOR will generally be possible for organic powder samples.

EXPERIMENTAL

The experiment was carried out with our homebuilt *field-cycling* spectrometer (*12*). The main part of the spectrometer is a rapidly switched solenoid coil into which the tail of a liquid helium cryostat fits. The problems in designing a field-cycled ENDOR probehead are the limited space in the cryostat and the collinearity of the external magnetic field and the cryostat axis. Therefore, the dimensions of the resonator and the coupling assembly are critical. Commercially available EPR probeheads cannot be used.

We chose a bridged loop–gap resonator (*15*) in our experiments because of its small dimensions and its good transparency for radiofrequency irradiation. The resonator was handmade by chemical deposition of silver on a quartz glass tube. The previously published method (*6*) was modified: The quartz glass tube was now allowed to stand for 72 h in an aqueous silver nitrate solution at room temperature with potassium sodium tartrate as the reducing agent. Quartz glass tubes of 12 mm length were cut from 702 PQ EPR tubes obtained from Wilmad. By the two methods presented in (*6*), we obtained the best signal-to-noise ratio with resonators whose structure was scratched after the deposition. The outer structure was scratched using stereoscopic magnifying glasses and a sharp knife. The inner structure was formed with a tool (Fig. 4) made from a steel rod with the same diameter as the inner diameter of the bridged loop–gap resonator.

The probehead (Fig. 5) includes a 14-turn ENDOR coil which is wound around a cylindrical Rexolite support and is fixed by a Teflon ribbon. The bridged loop–gap resonator inside the ENDOR coil is aligned perpendicular to the axis of the field-cycling solenoid and supported by a movable Rexolite holder. Impedance matching is performed at room temperature by moving the resonator. This can be done by rotating the resonator with its holder and by moving the complete structure of the resonator, resonator holder, ENDOR coil, and ENDOR coil holder. We cannot vary the coupling in liquid helium due to the limited space in the cryostat.

Figure 6 shows the block diagram of the field-cycled ENDOR spectrometer. The complete experiment is controlled

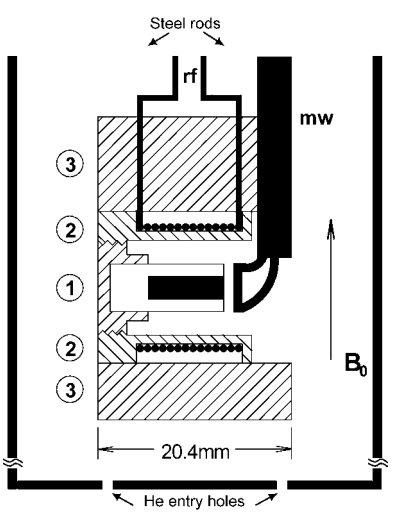

FIG. 5. Probehead for pulsed field-cycled ENDOR: (1) rotatable Rexolite holder for the bridged loop–gap resonator; (2) Rexolite ENDOR coil support; (3) Rexolite enclosure. Parts 1 and 2 of the probehead are movable within this enclosure. The probehead is fixed inside a stainless steel housing with entry holes for liquid helium.

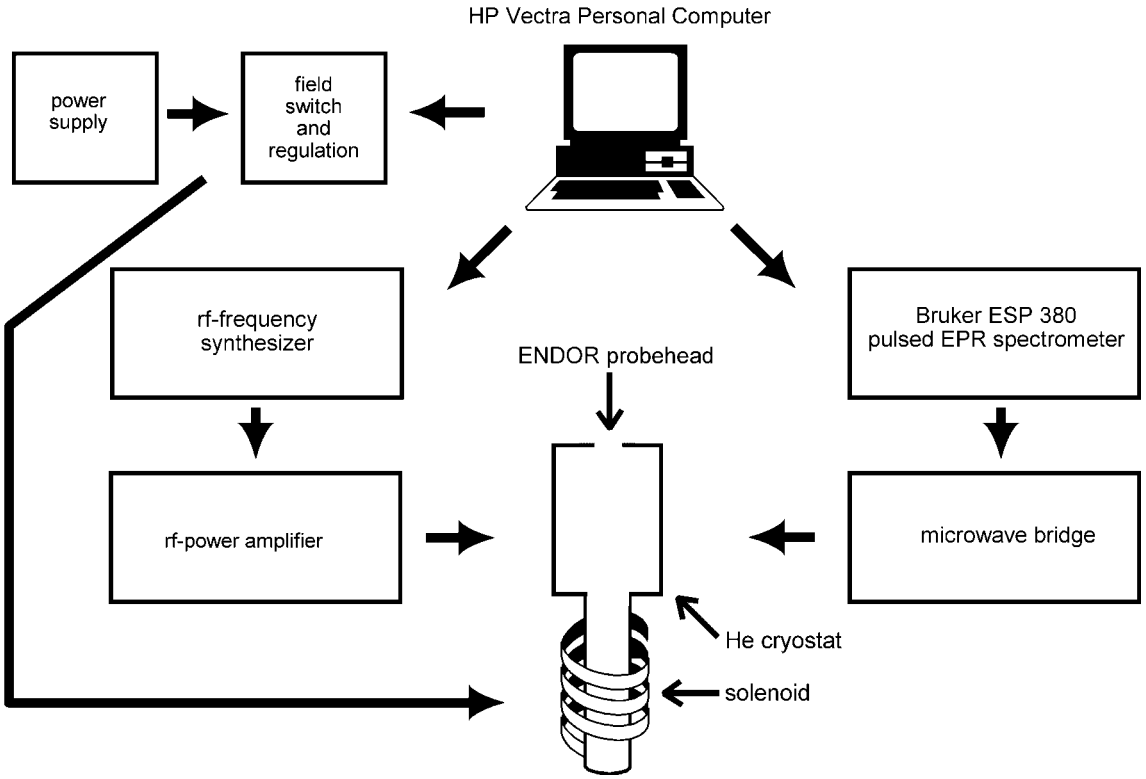

FIG. 6. Block diagram of the field-cycled ENDOR spectrometer (see text).

by a HP Vectra personal computer. This PC controls the field switch, the field regulation unit, and the radiofrequency generator, and it triggers the Bruker ESP 380 spectrometer. All experiments were performed with low-power microwave pulses, because we do not have a traveling-wave tube amplifier. A 50 W RF power amplifier was used for the ENDOR excitation.

As mentioned before, the field-cycling part of the spectrometer was substantially improved. The former solenoid used for the experiment in Fig. 2 was made of water-cooled hollow copper wire. A maximum field of 0.32 T was generated by this coil. The inner diameter of 56 mm led to a diameter of only 24 mm for the probehead in the liquid helium glass cryostat used for this experiment. No helium pump could be employed because of the liquid helium capacity of just 2 L. The new coil used for the experiment of Fig. 3 was built by F. Noack's group (University of Stuttgart, Germany). This coil is of a different design (*16*). It consists of four concentric aluminum tubes with an insulating helical groove of variable pitch cut into each of them. The coil is cooled by a perfluorated polyether as coolant (Galden, Ausimont, Milan) pumped with high flow rate (200 L/min). The complete frequency range of a Bruker X-band microwave bridge can be used for EPR due to the maximum field of 0.43 T generated by this coil. The inner coil diameter of 65 mm accommodates the tail of a commercial stainless steel helium bath cryostat. The cryostat was specially designed by Magnex Scientific for field-cycling experiments. The copper shield in the tail of the cryostat is slit to avoid the induction of eddy currents during the cycling. There is enough space inside this cryostat for the microwave and RF assembly shown in Fig. 5.

Helmholtz coils made of one turn of copper strips were used to compensate the stray magnetic field in the laboratory to less than 0.004 mT.

ACKNOWLEDGMENTS

Dr. S. Becker and Dr. J. Struppe (University of Stuttgart) made the field-cycling coil and gave us many useful hints for the construction of the cooling equipment. We are grateful to one of the referees and to P. Höfer (Bruker Analytik GmbH, Rheinstetten) for helpful and critical comments concerning the obtained spectra. Financial support from the Deutsche Forschungsgemeinschaft is gratefully acknowledged.

REFERENCES

1. Y. S. Lebedev, High-frequency continuous-wave electron spin resonance, *in* "Modern Pulsed and Continuous-Wave Electron Spin Resonance" (L. Kevan and M. K. Bowman, Eds.), pp. 365–404, Wiley, New York (1990).
2. R. Bramley and S. J. Strach, Electron paramagnetic resonance spectroscopy at zero magnetic field, *Chem. Rev.* **98,** 49–82 (1983).
3. A. Abragam, Une nouvelle méthode pour la polarisation des noyaux atomiques, *C. R. Acad. Sci.* **242,** 1720–1722 (1956).
4. D. B. Zax, A. Bielecki, K. W. Zilm, A. Pines, and D. P. Weitekamp, Zero-field NMR and NQR, *J. Chem. Phys.* **83,** 4877–4905 (1985).

5. J. Krzystek, M. Notter, and A. L. Kwiram, Field-cycled electron nuclear double resonance, *J. Phys. Chem.* **98,** 3559–3561 (1994).
6. G. Sturm, A. Lötz, and J. Voitländer, Pulsed detection of the zero-field electron spin–lattice relaxation time, *in* "Extended Abstracts of the 28th Congress Ampere, Canterbury," pp. 256–257, 1996.
7. G. Sturm, A. Lötz, and J. Voitländer, Pulsed EPR with field-cycling and a bridged loop–gap resonator made by chemical deposition of silver, *J. Magn. Reson.* **127,** 105–108 (1997).
8. G. Sturm, D. Kilian, A. Lötz, and J. Voitländer, Pulsed field-cycled ENDOR spectroscopy, *in* "Proceedings of the Joint 29th Ampere–13th ISMAR International Conference, Berlin," pp. 216–217, 1998.
9. G. Sturm, D. Kilian, A. Lötz, and J. Voitländer, Field-cycled ENDOR spectroscopy, *EPR Newsl.* **10** (1), 6–9 (1991).
10. C. P. Slichter, *in* "Principles of Magnetic Resonance," pp. 219–246, Springer, Berlin (1989).
11. D. T. Edmonds, Nuclear quadrupole double resonance, *Phys. Rep.* **29,** 233–290 (1977).
12. J. Olliges, A. Lötz, D. Kilian, and J. Voitländer, Boron nuclear quadrupole couplings and localized electronic wave functions in the boron clusters *o*-carborane and *o*-silaborane, *J. Chem. Phys.* **103,** 9568–9573 (1995).
13. P. Höfer, Distortion-free electron-spin-echo envelope-modulation spectra of disordered solids obtained from two- and three-dimensional HYSCORE experiments, *J. Magn. Reson.* **111,** 77–86 (1994).
14. P. Höfer, Bruker Analytik GmbH, Rheinstetten, private communication, 1999.
15. S. Pfenninger, J. Forrer, and A. Schweiger, Bridged loop–gap resonator: A resonant structure for pulsed ESR transparent to high-frequency radiation, *Rev. Sci. Instrum.* **59,** 752–760 (1988).
16. K. H. Schweikert, R. Krieg, and F. Noack, A high-field air-core magnet coil design for fast-field-cycling NMR, *J. Magn. Reson.* **78,** 77–96 (1988).